07,01

Influence of the structural state on the elastic and microplastic properties of aluminum alloy AD1

© M.V. Narykova, B.K. Kardashev, V.I. Betekhtin, A.G. Kadomtsev, A.I. Lihachev, O.V. Amosova

Ioffe Institute,
St. Petersburg, Russia

E-mail: Maria.Narykova@mail.ioffe.ru

Received July 3, 2023
Revised July 3, 2023
Accepted July 4, 2023

The results of a study of aluminum alloy AD1 in four structural states before and after severe plastic deformation are presented. Both the initial coarse-grained state (supply state) and three fine-grained states, which differ from each other in the method of obtaining, are considered. Elastic and microplastic properties (modulus of elasticity, decrement of elastic vibrations, microplastic deformation) were determined by the acoustic method of a composite vibrator. It is shown that the modulus of elasticity changes to a large extent under the influence of the evolution of internal stresses; the attenuation of ultrasound after severe plastic deformation increases due to an increase in the area of grain boundaries. Key words: AD1 aluminum, modulus of elasticity, microcrystalline aluminum, decrement of elastic vibrations, microplastic deformation.

Keywords: aluminum AD1, modulus of elasticity, microcrystalline aluminum, decrement of elastic vibrations, microplastic deformation.

DOI: 10.61011/PSS.2023.08.56580.139

1. Introduction

Aluminum alloys are widely used in various industries, which is of interest for further improving their strength properties and increasing the service life of products made of this alloy. One of the ways to improve mechanical properties are approaches based on intensive plastic deformation (IPD) [1]. Thermal and deformation processing in the IPD process allows creating a textured structure, changing the phase composition, grain sizes, distribution of grain boundaries, defect density [2,3]. However, it is difficult to predict the magnitude of the change in mechanical properties, since it is necessary to take into account many structural factors, especially if the alloy has a complex composition. Aluminum grade AD1 contains a small amount of impurities, so this alloy can be successfully used as a model material in the development of new technologies. The available impurities can contribute to the thermal and mechanical stability of ultrafine-grained materials obtained by the methods of IPD [4,5].

Thermomechanical processing developed in [6], consisting in a combination of various types of rolling, allows obtaining long-length blanks. This method was successfully implemented to produce titanium with a homogeneous ultrafine-grained structure and high mechanical properties [7] and was used for the first time to create an ultrafine-grained structure in the studied aluminum.

It is known that the modulus of elasticity (Young's modulus) allows characterizing the stress level in structural elements. One of the most accurate methods for determining the elastic characteristics of solids is the acoustic method. The use of this method for the study of elastic and microplastic properties is also of interest for studying the causes of changes of these properties. The main factors affecting their magnitude include the density of dislocations [8], the formation of microdiscontinuities [9] and internal stresses [10]. An important structural factor for polycrystals is the grain size and the presence of boundaries between them.

The results of structural and acoustic studies of aluminum AD1 before and after IPD are compared in this paper. The results of the study allow expanding the current understanding of the properties of ultrafine-grained materials.

2. Samples and methods

The study was conducted on technical aluminum grade AD1, the elemental composition of which according to the datasheet contains up to 0.3 wt.% Fe, up to 0.3 wt.% Si, up to 0.15 wt.% Ti, up to 0.1 wt.% Zn, up to 0.05 wt.% Cu, up to 0.05 wt.% Mg, up to 0.025 wt.% Mn and up to 0.05 wt.% of other impurities.

The aluminum alloy was presented when delivered (initial condition) in the form of a round bar with a diameter of 30 mm. Two states were formed according to the mode of mechanical-thermal treatment developed for the formation of a submicrocrystalline (SMC) structure in titanium [11], hereinafter referred to as SMC-1 and SMC-2. Mechanical heat treatment consisted of several stages combining cross rolling and longitudinal rolling. After rolling, the bars had the shape of a rod of circular cross-section with a diameter of about 7 mm. The difference in the process of forming a submicrocrystalline structure for these two states consisted

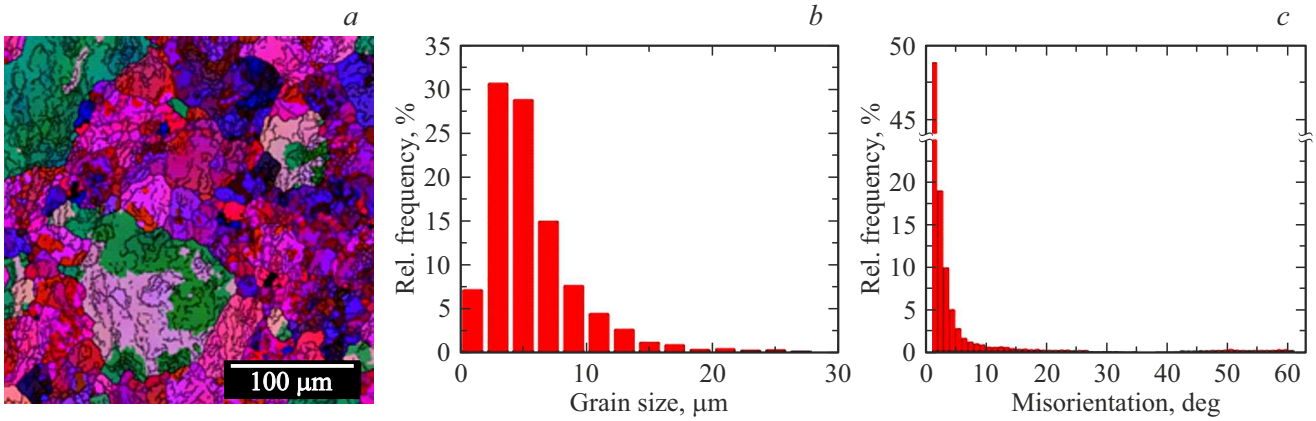

Figure 1. Microstructure of aluminum alloy AD1 in the original condition (delivery state): Euler angle distribution map (*a*), grain size histogram (*b*) and grain boundary misorientation angle histogram (*c*).

in the temperature during finishing rolling: SMC-1 was produced at room temperature, SMK-2 was produced with an additional cooling in liquid nitrogen. A recrystallized microcrystalline state hereinafter referred to as MC was formed from SMC-1 by annealing at 250° during one hour.

Structural studies were carried out using a scanning electron microscope (SEM) JSM 7001F (JEOL, Japan) with a HKL Nordlys EBSD detector (Oxford Instruments, England). Maps of crystallographic orientations were obtained, grain size histograms and grain boundary histograms at disorientation angles were constructed using electron backscatter diffraction (EBSD) method. MultiPrep 8 polishing system (Allied, San Francisco, CA, USA) was used for the preparation of polished sections with a sequential reduction of the abrasive grain for mechanical grinding of the section. The final polishing of the cross-section surface was carried out by a beam of argon ions using 1061 SEM Mill system of ion milling and polishing (Fischione, Export, PA, USA).

Elastic and microplastic properties (Young's modulus E, elastic vibration decrement δ and microplastic flow stress σ were determined using the resonance method of a composite piezoelectric vibrator [12]. Samples of rectangular cross-section $1.4 \times 2.5\,\mathrm{mm}^2$ with a length of 25 mm were taken from the central part of round rods. The tests were carried out at a frequency of about 100 kHz in a wide range of oscillatory strain amplitudes ε, including linear (amplitude-independent) and nonlinear (microplastic) regions. The modulus of elasticity was calculated using the formula

$$E = 4\rho \cdot l^2 \cdot f^2, \qquad (1)$$

where l — length, ρ — sample density, f — oscillation frequency. Relative error of measurement of the natural frequency of the sample by the double vibrator method $\sim 10^{-3}$; relative error of the measurement of the modulus of elasticity $\sim 4 \cdot 10^{-3}$.

Microplastic property data are obtained from measurements of the modulus E and the decrement of elastic vibrations δ, when at large ε nonlinear, amplitude-dependent damping $\delta_\mathrm{h} = \delta - \delta_\mathrm{i}$ occurs in the sample material and the amplitude-dependent defect of Young's modulus $(\Delta E/E)_\mathrm{h} = (E - E_\mathrm{i})/E_\mathrm{i}$. Here E_i and δ_i — the values of Young's modulus and decrement measured at small amplitudes, where the modulus E and decrement δ do not yet depend on ε.

Acoustic measurements in a wide range of amplitudes make it possible to evaluate the mechanical (microplastic) properties of materials in the coordinates „stress-strain" familiar to conventional mechanical tests. To do this, the values of oscillatory stress amplitudes $\sigma = E \cdot \varepsilon$ (Hooke's law) are measured along the ordinate axis, and nonlinear inelastic deformation $\varepsilon_d = \varepsilon \cdot (\Delta E/E)_\mathrm{h}$ is measured along the abscissa axis.

The density of wire samples was determined by hydrostatic method using analytical scales Shimadzu AUW 120D (Shimadzu Corporation, Japan) with specific gravity measurement kit SMK-301. This method was used not only to determine the integral density of each of the samples ρ, but also for the relative change in the density of the samples $\Delta\rho/\rho$ after various treatments. The relative error in determining the density is 0.02%.

3. Experimental results and discussion

3.1. Structural studies

In the initial state (before rolling), the structure is mainly represented by grains from 2 to 7 μm (Fig. 1) with a predominance of small-angle grain boundaries.

A structure was formed after rolling to the SMC-1 state with an average grain size in cross-section of about 470 nm and a relatively small ($\sim$ 10%) fraction of grains larger than 1 μm (according to transmission electron microscopy data). More than 50% of the grains have a size from 200 to 800 nm. There is a moderately pronounced radial texture with a texture axis parallel to the normal to the plane (110) directed along the rolling direction.

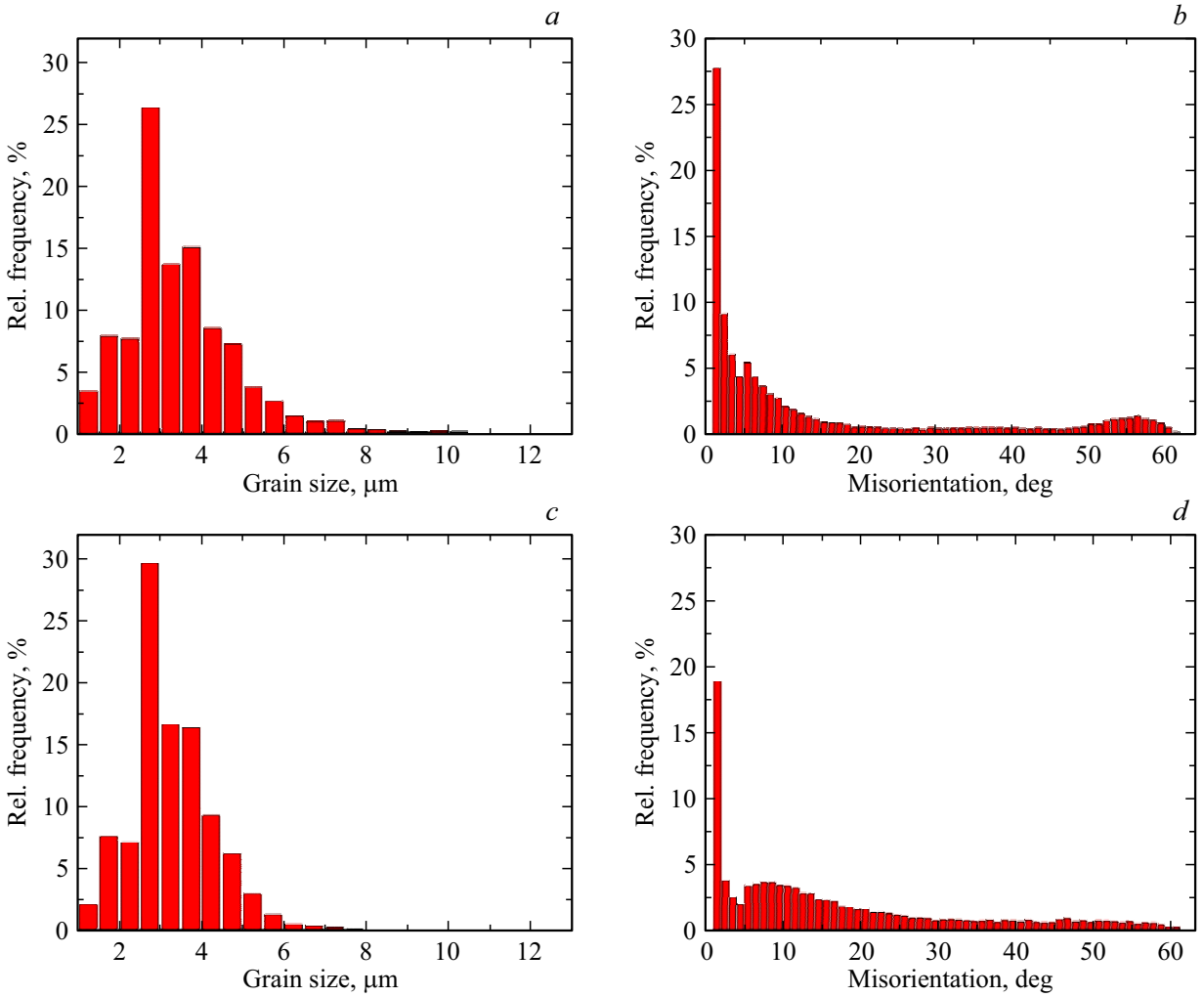

Figure 2. Microstructure of aluminum alloy AD1 in SMC-1 state — grain size distribution — *a, c* and grain boundary misorientation angles — *b, d* (*a, b* — center, *c, d* — edge).

The use of liquid nitrogen at the final stage of rolling to form the SMC-2 structure resulted in a slight increase in the average grain size in cross-section — up to 500 nm. The size of large grains here did not exceed 1.8 μm, and in general the structure turned out to be more homogeneous compared to the state SMC-1.

EBSD analysis was performed in the center and at the edge of the rod (longitudinal section along the direction of rolling) to study the uniformity of the microstructure after rolling. The grain size distribution over the cross section of the rod did not reveal any features (Fig. 2): the structure in SMC-1 and SMC-2 is represented by grains from several hundred nanometers to 10 μm. The grains have a somewhat elongated shape in the direction of rolling.

Some differences were obtained when the dependencies of the misorientation angles for the central part of the rod and its edge were constructed (Fig. 2). There is a significant proportion of small-angle boundaries (with disorientation up to 10°) and there is a small peak with disorientation 50–60° in the central part of the sample. The edge of the bar is also characterized by the presence of predominantly small-angle intergrain boundaries, but disorientation in the range 25–60° has no features.

The average grain size in cross-section is about 1.5 μm in the recrystallized MC state, according to transmission electron microscopy data. In addition, small maxima were found on grain size histograms in the region of sizes 2 and 4 μm, the sizes of individual grains reach 7 μm.

3.2. Elastic and microplastic properties

The main results of experimental studies of this work are provided in Fig. 3 and 4 and in the Table.

Fig. 3 shows the amplitude dependences of the Young's modulus E and the decrement δ for various structural states of the aluminum alloy AD1. The dependences $E(\varepsilon)$ and $\delta(\varepsilon)$ were measured sequentially with increasing and decreasing amplitude at room temperature. Acoustic deformation diagrams $\sigma(\varepsilon_d)$ are plotted on Fig. 4 based on the data for $E(\varepsilon)$ shown in Fig. 3 and taken at the

Average grain size, density ρ, Young's modulus E_i, amplitude-independent decrement δ_i, micro-flow stress σ_s under inelastic deformation $\varepsilon_d = 5.0 \cdot 10^{-8}$ and macroscopic yield strength σ_f for various states Al-AD1

Al-AD1 (state)	Size grains, nm	ρ, g/cm^3	E_i, GPa	δ_i, 10^{-5}	σ_s, MPa	σ_f, MPa
Initial	5000	2.7004	69.20	12.4	14.5	–
SMC-1	470	2.6970	69.33	34.1	17.0	128
SMC-2	500	2.6970	68.80	30.0	17.8	136
MC	1500	2.6989	68.16	12.3	11.4	90

first amplitude increment. The table shows the values of the average grain size, density ρ, Young's modulus E_i and amplitude-independent decrement δ_i measured at small amplitudes, and micro-fluidity stress σ_s at fixed value of inelastic deformation $\varepsilon_d = 5.0 \cdot 10^{-8}$ and macroscopic yield strength σ_f.

When considering the data obtained, the most obvious effect of the IPD (grain size) is demonstrated by the decrement δ and the microplastic flow stress σ (similar dependences for the aluminum alloy Al-0.2%Sc were obtained by the authors earlier [13]).

Fig. 3 and the table show that the amplitude-independent decrement δ_i increases markedly with a decrease in grain size during the transition from the initial state to SMC-1

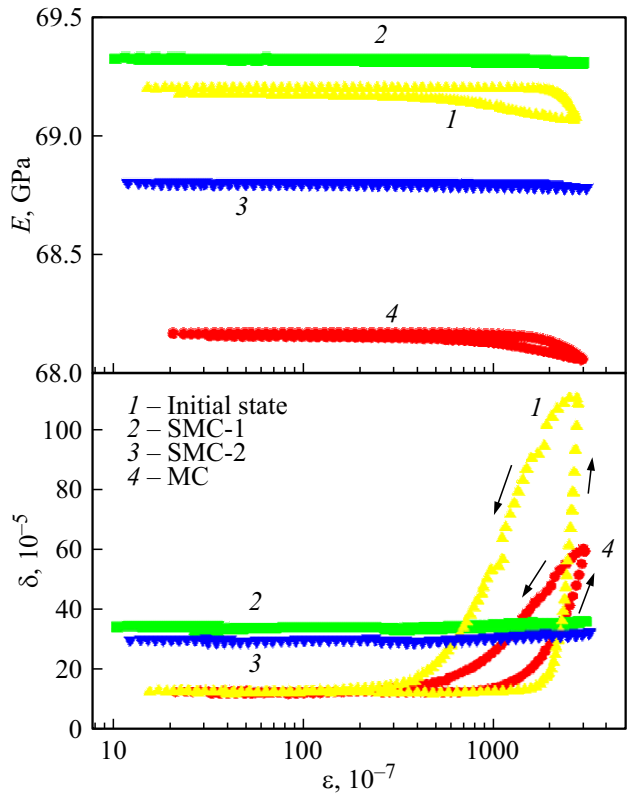

Figure 3. Amplitude dependences of Young's modulus E and decrement δ for AD-1 aluminum samples in various structural states. Measurements are performed at room temperature.

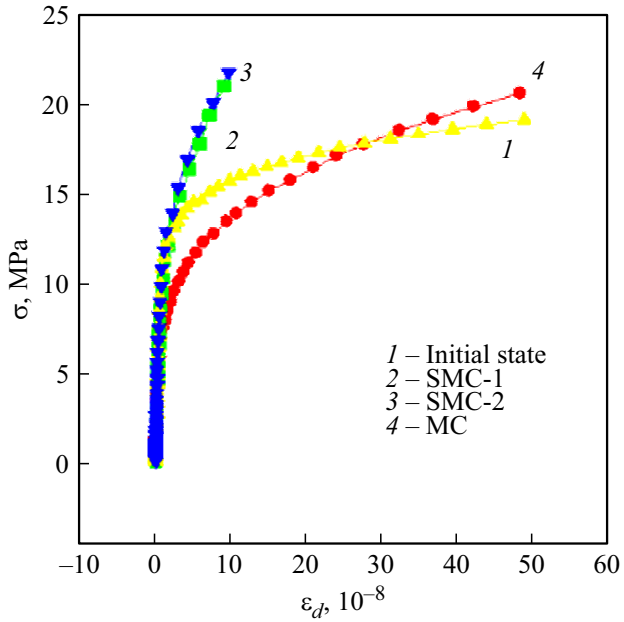

Figure 4. Diagrams of microplastic deformation of AD-1 aluminum samples in various structural states.

and decreases with its increase from SMC-1 to MC. It is interesting to note that δ_i also decreases with a slight increase in grain size in SMC-2 to 500 nm (470 nm in SMC-1). This effect can be explained as follows: the smaller the grain size, the larger the area of the boundaries between the grains on which the ultrasound energy is dissipated.

The stresses σ (Fig. 4) and σ_s (Table) also increase with the decrease of the grain size. This, apparently, is due to the fact that there are fewer carriers of inelastic deformation (dislocations) in small grains after the IPD. Therefore, a higher stress is needed to achieve the same fixed strain $\varepsilon_d = 5.0 \cdot 10^{-8}$ (Table).

It is interesting to note that a similar behavior of macromechanical properties was revealed as a result of standard mechanical tests. Thus, the yield strength of σ_f (Table) was 90, 128 and 136 MPa respectively, in MC, SMC-1 and SMC-2 states. As can be seen from the table, the nature of changes of mechanical properties at the macro and micro levels is consistent.

When comparing the curves $\sigma(\varepsilon_d)$ for coarse-grained states (delivery and MC), it is seen (Fig. 4) that at small ε_d the level σ for MC is less, and at large ε_d — greater. This may be due to the different distribution of dislocation segments by length in both materials. Indeed, according to the theory of amplitude-dependent internal friction [8,12], the type of dependences of the decrement and the modulus defect on the amplitude is formed by the point centers of dislocation fixation and their distribution along the dislocation line. It is possible to note here the synchronous behavior of both $\sigma(\varepsilon_d)$ in Fig. 4, and $\delta(\varepsilon)$ in Fig. 3 when comparing both materials.

MC and original state show a hysteresis on the graph $\delta(\varepsilon)$ while ultrafine-grained states virtually do not demonstrate any hysteresis. When the amplitude dependences do not coincide with each other with a sequential increase and decrease in amplitude, it can be assumed that the defects that serve as effective pinning points for dislocation movements are shifted during the measurement process, their distribution along dislocation lines changes noticeably [12].

Young's module behaves differently. Fig. 3 and the table show that the values of the module E_i are noticeably different for each of the states. The formation of the SMC-1 structure led to a slight increase in the modulus relative to the initial state — from 69.20 to 69.33 GPa. The application of additional cooling during rolling on the SMC-2 reduced the module to 68.80 GPa (relative to the initial state of 69.20 GPa). The value of the modulus E_i significantly decreased after recrystallization annealing and was even lower than in the delivery state — to 68.16 GPa.

Such a complex behavior of the module can be explained by a number of reasons. As is known, the introduction of fresh dislocations into the sample as a result of plastic deformation should decrease the modulus E_i and increase the decrement δ_i [8,12]. The module can decrease also as a result of the discontinuities in the material, which are directly manifested by a decrease of density according to the formula (1). The growth of E_i with an increase of δ_i is explained by an increase of the level of internal stresses [10,14]. Thus, the modulus changes observed in this work as a result of IPD and heat treatment can be associated with dislocations, the density of the sample material and the evolution of internal stresses. The predominant impact of high internal stresses undoubtedly takes place during the formation of the SMC-1 state, where the highest modulus is observed.

4. Conclusion

The formation of an ultrafine-grained structure in technical aluminum AD1 resulted in a change of elastic and microplastic properties. There is a noticeable increase of the decrement and stress of the microplastic flow in the ultrafine-grained state. A noticeable effect of the level of internal stresses on the change in the Young's modulus was found: the higher value in the SMC-1 state is undoubtedly attributable to the impact of long-range internal stress fields.

Acknowledgments

The authors thank professor Yu.R. Kolobov for thermomechanical processing of AD1 samples.

Funding

EBSD studies were carried out using the equipment of the Federal Center of Collective Use „Materials science and diagnostics in advanced technologies".

Conflict of interest

The authors declare that they have no conflict of interest.

References

[1] M.A. Meyers, A. Mishra, D.J. Benson. Prog. Mater. Sci. **51**, *4*, 427 (2006).
[2] Y. Cao, S. Ni, X. Liao, M. Song, Y. Zhu. Mater. Sci. Eng. R **133**, 1 (2018).
[3] J. Gubicza. Mater. Trans. **60**, *7*, 1230 (2019).
[4] I. Saxl, L. Ilucová, M. Svoboda, V. Sklenička, V.I. Betekhtin, A.G. Kadomtsev, P. Král. Mater. Sci. Forum **567**, 193 (2007).
[5] Z. Horita, T. Fujinami, M. Nemoto, T.G. Langdon. J. Mater. Proc. Technol. **117**, *3*, 288 (2001).
[6] Y.R. Kolobov. Russ. Phys. J. **61**, *4*, 611 (2018).
[7] V.I. Betekhtin, Y.R. Kolobov, M.V. Narykova, B.K. Kardashev, E.V. Golos, A.G. Kadomtsev. ZhtF **81**, *11*, 58 (2011). (in Russian).
[8] G. Gremaud. Mater. Sci. Forum **366**, 178 (2001).
[9] R. Chaim, J. Hefetz. Mater. Sci. **39**, 3057 (2004).
[10] B.K. Kardashev, O.A. Plaksin, V.A. Stepanov, V.M. Chernov. Phys. Solid State **46**, *8*, 1449 (2004).
[11] M.B. Ivanov, A.V. Penkin, Y.R. Kolobov, E.V. Golos, D.A. Nechayenko, S.A. Bozhko. Deformatsiya i razrushenie materialov, **9**, 13 (2010). (in Russian).
[12] S.P. Nikanorov, B.K. Kardashev. Uprugost' i dislokatsionnaya neuprugost' kristallov. Nauka, M., (1985). (in Russian). 254 p. (in Russian).
[13] V.I. Betekhtin, V. Sklenicka, I. Saxl, B.K. Kardashev, A.G. Kadomtsev, M.V. Narykova. FTT **52**, *8*, 1517 (2010). (in Russian).
[14] V.I. Betekhtin, A.G. Kadomtsev, B.K. Kardashev. FTT **48**, *8*, 1421 (2006). (in Russian).

Translated by A.Akhtyamov